DESIGN AND TEST OF A FLAPPING WING MICRO-AERIAL VEHICLE

A Major Qualifying Project Report

submitted to the Faculty of the

WORCESTER POLYTECHNIC INSTITUTE

in Partial Fulfillment of the requirements for the

Degree of Bachelor of Science

in Aerospace Engineering

by

Andrew Joseph Firenze

Trae Lee Jennette

Nishan Srishankar

Date: March 6th, 2014

Approved by:

Professor Maria Chierichetti, Major Advisor

Professor Michael Demetriou, Co-Advisor

Aerospace Engineering Program

Mechanical Engineering Department, WPI

ABSTRACT

The objective of this project is to design, fabricate and test a Flapping Wing Micro Aerial Vehicle (MAV) with hovering capability. The MAV is designed to bio-mimic hummingbird flight, in which the wings flap in a plane perpendicular to the horizontal. Aerodynamic lift is created from the interaction between the wings and the vortex generated by the previous stroke (wake-capture motion). The team designed, manufactured and assembled an initial static prototype. The final design is characterized by a wing span of 36 cm and a weight of 41 g. The wings have been manufactured using monokote reinforced with carbon fiber, while the chassis and drive train have been 3-D printed based on thermoplastics.

AUTHORSHIP

The table prepared below outlines the division of work amongst all team member of the Flapping Wing Micro Air Vehicle (flapping MAV) Major qualifying project. The student who was prepared or presented the physical product included in the corresponding section of the report has his initials placed in the "Creator" column. The student who wrote the section corresponding to the physical product has his initials located in the "Author" column. The student who peer-reviewed that section of the report has his initials located in the "Editor" column. The abbreviation of names are as follow:

TJ: Trae Jennette

NS: Nishan Srishankar

AF: Andrew Firenze

	Creator	Author	Editor
Chapter 1: Introduction			
1.1 Literature Review	-	NS	TJ/AF
1.2 Design Objectives	-	NS	TJ/AF
1.3 Wake Capture	-	NS	TJ/AF
1.4 Organization of Work	-	NS	TJ/AF
Chapter 2: Estimate of Aerodynamic Forces			
2.1 Instantaneous Lift Equation	NS	NS	TJ/AF
2.2 Lift Equation for Hover	NS	NS	TJ/AF
2.3 Flapping Wing Motion	AF	AF	TJ/AF
Chapter 3: Design			
3.1 Chassis & Drivetrain Design	TJ	AF	TJ/AF
3.2 Final Design	TJ	AF	TJ/AF
3.3 Part Specification	TJ	TJ	TJ/AF
Chapter 4: Manufacturing			
4.1 Wing Manufacturing	TJ	TJ	TJ/AF
4.2 Chassis & Drivetrain Manufacturing	TJ	TJ	TJ/AF
Chapter 5: Vibration Analysis	AF	AF	TJ
Chapter 6: Conclusion & Remarks	TJ	TJ	All

TABLE OF CONTENTS

LIST OF FIGURES

LIST OF TABLES

CHAPTER 1: INTRODUCTION

The main goal of this MQP is to design a flapping-wing micro aerial vehicle (MAV) that bio-mimics the hovering capabilities of hummingbirds, with a maximum weight of 100 grams and a maximum wing span of 40 centimeters. Additionally, the MAV should be able to perform a set of motions: vertical take-off, motion in X, Y and Z planes, hover and descent. The following chapters will go through the iterative engineering design process required to obtain the end goal, specifically operating parameters, external dimensions, detailed design phases, material requirements, and manufacturability and test requirements.

1.1 LITERATURE REVIEW

Humans have always been interested in mirroring bird flight. From the Greek fables of Daedalus and Icarus to Leonardo Da Vinci's drawings of ornithopters and Otto Lilienthal's vision of gliders, the first few centuries of flapping-wing flight research has been focused on human transport. One example of flapping-flight research that is currently being conducted deals with micro-aerial vehicles. According to the Defense Advanced Research Projects Agency (DARPA), an MAV is a maneuverable robot that has a maximum gross weight of 100 grams [1,2].

Progress in aerodynamics, electronics, micro-electromechanical systems (MEMS), manufacturing and feedback systems have allowed for development of MAV's for use especially in military and research applications, ousting traditional fixed and rotary wing vehicles. Despite this, complete autonomy has not been achieved in flapping wing MAVs because the aerodynamics, kinematics, guidance, navigation and control are more complex than that of fixed wing aircraft.

Flapping-wing MAVs operate at relatively low velocities and Reynolds numbers therefore flow field characteristics are important. Furthermore, wing and tail kinematics, aerodynamics, and weight constraints for actuators and power need to be taken into consideration. The complexity of this design process can be acknowledged, as it becomes clear that no artificial flapping-wing MAV has matched the performance of birds in nature, and it is for this reason that nature serves as a tool to understand how a flapping-wing MAV should ideally operate. One important fluid flow parameter that needs to be understood is whether the flow type is laminar or turbulent. The transition between laminar and turbulent flow depends on Reynolds number, which relies on the design of the micro-aerial vehicle. Most small birds fly with velocities resulting in Re>20000 leading to predominantly turbulent flow over their wings. Flows around hummingbirds for instance have 5,000<Re<30000 [4,6]. These Reynold's number ranges coincide with a laminar-turbulent fluid flow transition. Due to difficulty in understanding the biology of hummingbirds' wings, the related aerodynamic aspects are still debated. Elimelech and Ellington, argued that this transitional flow regime is vital in creating an unsteady flow field (involving vortex-shedding and reattachment), which, based on experimentation performed, seems to occur in hummingbird wings during forward flight and hover [5].

There are two main methods for hovering flight in nature: one seen with hummingbirds and one seen with dragonflies, as shown in Figure 1. Hummingbirds use wake capture and horizontal stroke-plane hovering. This involves the wings flapping in a plane that is parallel to the horizontal (ground). On the other hand, dragonflies use the clap-and-fling method, and inclined stroke-plane hovering, which involves the wings beating in a plane that is at an angle inclined to the horizontal.

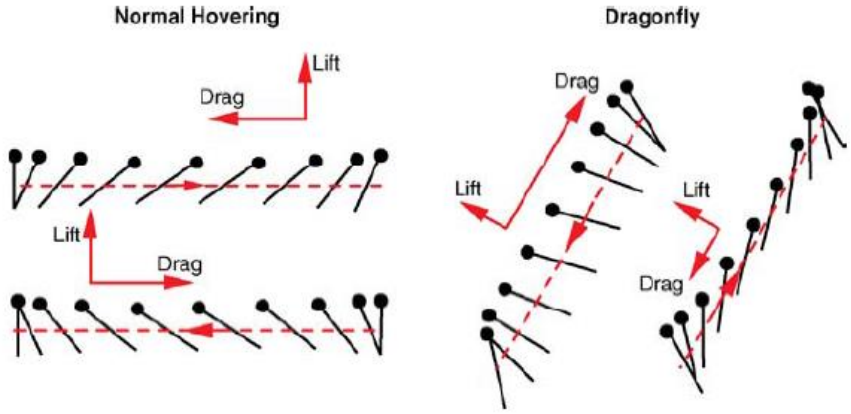

Figure 1: Two Hovering Styles. (A. Left): Normal Hovering in a Horizontal Stroke Plane- Hummingbirds. (B. Right): Hovering in an Inclined Plane- Dragonflies [Copyright: Wang, Z. Jane. 2005]

Designing a bio-mimetic flapping wing MAV involves capturing complex motions of the wing, especially in hover. Flapping wings can have four Degrees of Freedom (DOF) if a rigid body assumption is made. Two DOFs allow us to specify the orientation of the leading edge of the wing in space, and the third DOF specifies the rotation of the wing about the leading edge. A fourth DOF, which will not be considered within the scope of this project, accounts for flexible wings and allows the wing tip to flex relative to the wing root. For this project, we define a 3-DOF wing which includes a stroke angle (Φ), elevation angle (θ) and angle of attack (α).

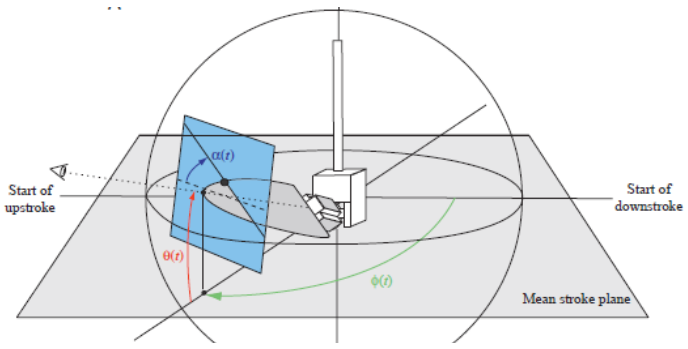

Figure 2: Wing Position defined by the Stroke Angle, Elevation angle and Angle of Attack

As shown in Figure 2, these three angles define the wing position at any instant of time. The stroke angle is the position of the wing in the stroke plane from down-stroke to upstroke. The elevation angle is the angle that the wing half-span makes with the stroke plane. The angle of attack is the angle of the wing with respect to the free-stream velocity.

From the literature review conducted, it was found that the main parameter that needs to be taken into consideration is the Wing Loading, defined as the weight of the MAV divided by the wing span. As shown in Figure 3, birds and bats have a Wing Loading of approximately $20Nm^{-2}$ because of a very small mass that is offset by a relatively large wing area. Additionally the power-to-weight ratio dictates whether the MAV can "fly" i.e. if the motor is able to produce a torque (and hence power) to support the weight of the micro-aerial vehicle.

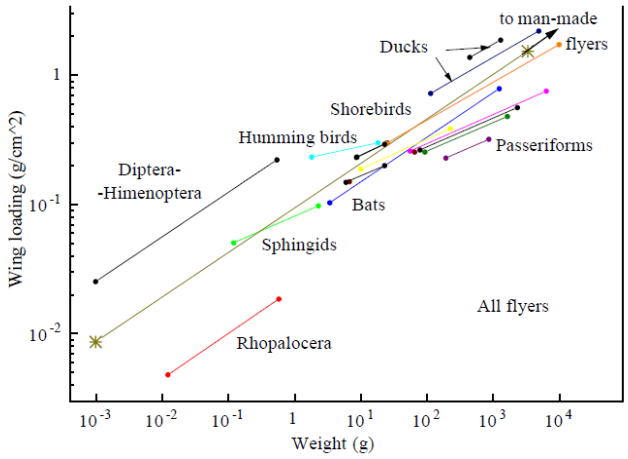

Figure 3: Wing Loading vs. Weight for Variety of Birds
[Copyright: Greenwalt. 1962]

Additionally, research into previous flapping-wing micro aerial vehicles gave an insight into the specifications and ball-park values to which the flapping-wing could be built to ensure design efficiency [6]. The main characteristics of previous designs are summarized in Table 1. Most of the previous flapping MAVs have two degrees of wing freedom, and have near equivalent wing spans and lengths, of around 33.1cm span and 25.5cm length. Based on initial weight and dimension estimates, the team's MAV would be much larger than previous designs, and hence would have a greater mass as well.

Name	**DOF**	**Weight (g)**	**Span (mm)**	**Length (mm)**
Wright State University	2	12.56	200.66	228.60
I-Fly	2	12.00	266.70	209.55
Delfly I	3	30.00	500.13	508.00
Delfly II	3	16.07	279.91	279.40
Delfly Micro	3	3.07	100.08	101.60
NPS Flier	2	12.40	269.24	180.09
Flytech Dragonfly	2	28.35	312.42	419.10
I-Fly Vamp/Wasp	2	13.00	266.70	215.90
Microbat (UF/ DARPA)	2	12.50	230.12	152.40
UMD Small Bird	2	9.30	342.90	203.20
UMD Bird Bird	2	27.90	571.50	266.70
UMD Jumbo Bird	2	38.00	635.00	297.18

Table 1: Characteristics and Specifications of Previous Flapping-Wing MAV's

This also leads to realizing that ornithopters could have three different wing configurations, each with different power requirements, lift outputs and flight effects: the

monoplane, biplane and tandem configurations [7]. The monoplane has a pair of flapping wings that flaps in phase about a common hinge. The biplane has two sets of wings placed on top of each other with each set of wings moving in antiphase. The last configuration has a tandem configuration, with two sets of wings placed along the length of the MAV (one wing set behind another). Table 2 shows the relative performances and flight characteristics.

	Monoplane	Biplane	Tandem
			
Average flight speed	2.35 m/s	1.40 m/s	1.36 m/s
Power consumption	0.75 W	0.69 W	1.00 W
Rocking amplitude	~80 mm	~0 mm	~0 mm

Table 2: Monoplane, Biplane and Tandem Wing Configurations [Copyright: Technical University of Delft]

As can be seen, the monoplane has the highest wing speed because of its high wing loading. Additionally, a monoplane with the same wing area as a biplane consumes less power, but would require an increase in size of the MAV.

1.2 DESIGN OBJECTIVES

Based on the research conducted, a set of objectives is shown in Figure 4.

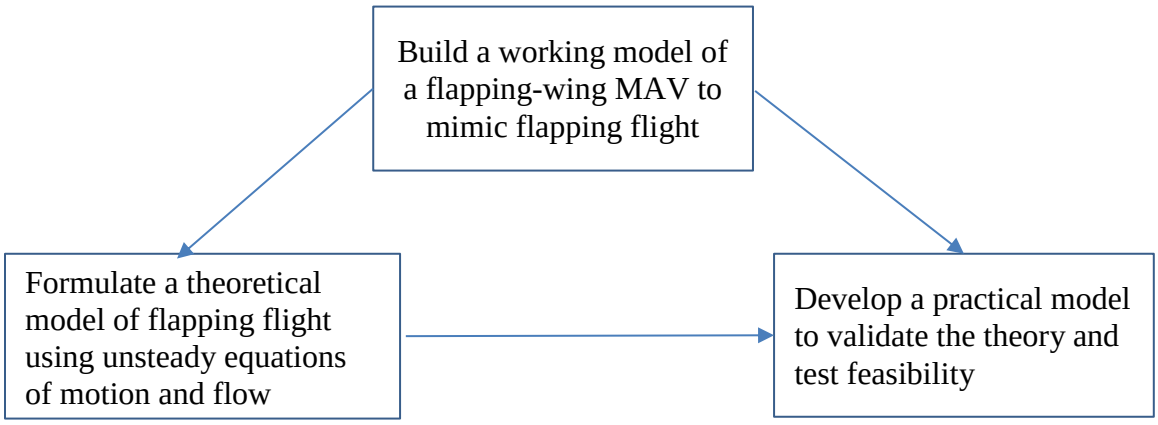

Figure 4: Basic Objective Analysis

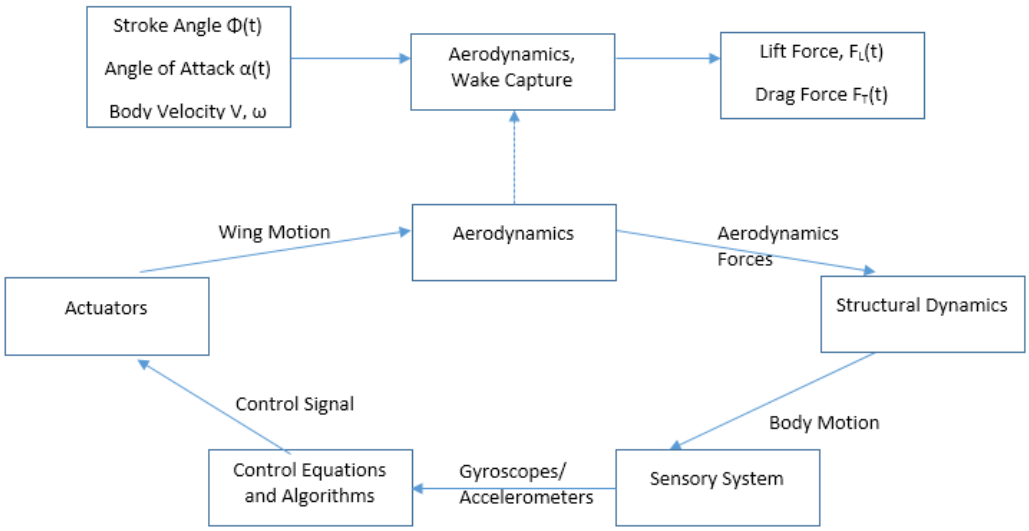

Figure 5: In-depth Systematic Flowchart to Fulfill Motion

The major challenges in creating a mechanical hummingbird MAV are:

- Predicting low Reynolds numbers and deriving a model for the unsteady aerodynamic loads, and wakes/ vortices.
- Designing a system characterized by strong fluid-structure interactions between the air-wing and air-fuselage boundaries.
- Fabricating micro-components given the overall dimensions of the MAV and the limitations of the possible fabrication methods based on material specifications.

1.3 WAKE CAPTURE

The previous MQP team that worked on the Flapping Wing MAV project utilized a clap-and-fling mechanism to provide aerodynamic lift [4,9,10]. The clap-and-fling mechanism involved the use of four wings. It works by the wings coming together at the end of each upstroke, also known as the 'clap'. The trailing edges of the wings still are connected after the clap, while the distance between leading edges of the wings keep increasing, which is referred to

as ‘fling’. When the wings start the down stroke, this effect induces a confined vortex at the leading edge of the wing, which in turn acts as a starting vortex for the other wing.

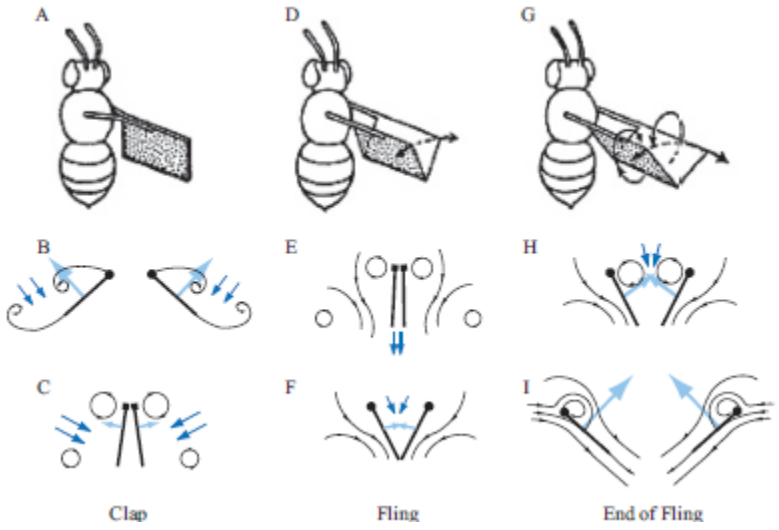

Figure 6: Clap and Fling Mechanism [23]

While both the wake capture and the clap and fling motions are both one-dimensional, the clap-and-fling mechanism showed that it requires a more complex flapping-mechanism in order to achieve the required wing motion while the kinematic system for wake capture is simpler. This is partly because MAV’s using the clap-and-fling mechanism require a four-wing setup to work, whereas MAV’s using the wake-capture require a two-wing setup.

Furthermore, even if the clap-and-fling mechanism is used by some insects to create a rotational airflow circulation, it is avoided by most insects and birds because permanent ‘clapping’ can damage the organisms’ wings. An alternative mechanism to provide aerodynamic lift to flapping wings is the wake capture motion. Wake capture exploits the back and forth motion of wings to cause an interaction with vortices of the prior strokes to generate lift.

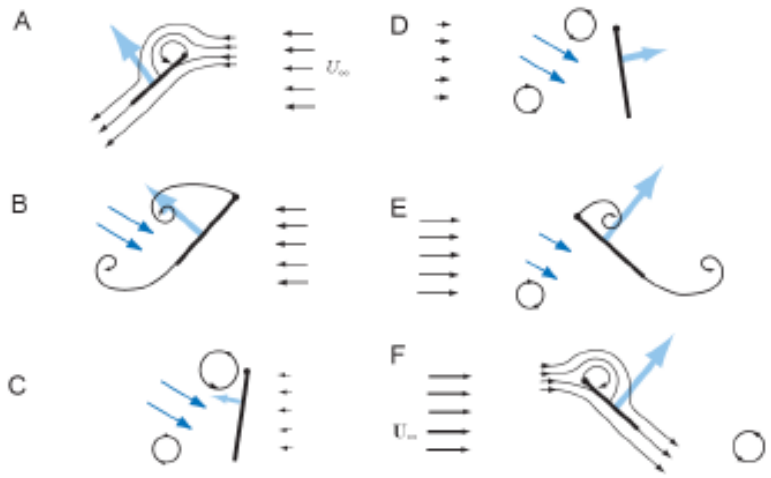

Figure 7: Wing-Wake Interactions

State	Description
A	Translational Phase
B	Wing starts the rotation around a chord-wise axis (before stroke reversal) causing both leading edge- and trailing edge- vortices
C	This rotation causes vortices as wing edges to be shed
D	The shed vortices are pushes against the wing, leading to a strong velocity field
E	The lift force is increased for the next half-stroke
F	The leading-edge vortex is reformed for the next translation

Table 3: Mechanism of Action for Wing-Wake Interactions

This mechanism is described in Figure 6 and Table 3. As the wing reverses strokes (A-C), it sheds the leading edge and trailing edge vortices, which induces a strong velocity field (the strength and orientation of this field depends on the position and strength of the two vortices). When the wing reverses direction, the enhanced velocity and acceleration fields interact with the wing, resulting in much higher aerodynamic forces.

Furthermore, this method of lift-generation allows for hovering capabilities (since the wing would reencounter wakes left behind in the previous stroke) unlike the clap and fling method.

The wing-wake interactions can be understood by the application of the following equations that describe how the generated aerodynamic forces relate to the characteristics of the flow [8].

$$F = -\rho \frac{d\gamma}{dt} + m \frac{dU}{dt} \quad (1)$$

$$\gamma = \int r \times \omega \, dR \Big\}_{R_\infty} \quad (2)$$

Notation	Meaning
F	Aerodynamic Forces acting on a solid body in a fluid (wing in air)
ρ	Fluid Density
m	Mass of fluid displaced by the solid body (air displaced by the wing)
U	Wing Velocity
γ	First moment of Vorticity
r	Position Vector
ω	Vorticity
dR	Element of area

Table 4: Breakdown of the Terms in the Aerodynamic Force and Vorticity Equations

Vorticity (ω) is a pseudo-vector that is the sum of the local angular velocities of a particular point in a fluid. Equation 1 summarizes all aerodynamic forces acting on a solid body

within a fluid, which in the case of our system, is the hummingbird in air. The first term evaluates the time-dependent changes in force due to the changes in the magnitude and distributions of the vorticity, during wing-wake interactions.

The second term in Equation 1 is the force created as an accelerating body displaces fluid. A wing can be approximated as a thin plate, which means the $m\frac{dU}{dt}$ term is negligible, and therefore the flapping flight components are all summarized in the first term of the equation. We have introduced this assumption because the thickness of our wings are >1% at all points span wise. The thickness of a wing is defined as the maximum thickness divided by the chord length and represented as a percentage. This means that the vorticity and the position vectors create the majority of aerodynamic forces on the wing.

1.4 ORGANIZATION OF THE WORK

After this introductory chapter, the details of the flapping wing design will be illustrated. Chapter 2 will describe the mathematical model for aerodynamic lift and drag as well as look into a potential lift equation for hover. Furthermore, it will contain an analysis of flapping wing motions, and the optimum wing motion for this project will be selected.

Chapter 3 will describe all the components that have been designed. In particular, it will show a SolidWorks model of the flapping MAV that will house all the required electronic components. In addition to this, vibration analyses will be conducted to ensure that any of the parts of the MAV will not resonate dangerously during the flapping motion.

One of the main aspects of this project is to obtain a tangible deliverable, from a virtual model. Chapter 4 will therefore describe the manufacturing process that will be divided into two

main parts, namely the creation of the wings and the rapid-prototyping of the chassis and the drive trains.

Chapters 5 describe the vibrational analysis performed on SolidWorks models to ensure that the components will handle stresses of flapping flight without failure.

Chapter 6 summarizes the experience that the team had during the fulfillment of this MQP, as well problems faced, and offers recommendations to subsequent teams that will work on this MQP.

CHAPTER 2: AERODYNAMICS

This section of the report outlines the mathematics behind creating a lift equation specific for our MAV, particularly for hover. We also analyzed potential flapping wing motions as researched in other projects and selected a motion that was efficient and could provide optimum lift.

2.1 INSTANTANEOUS LIFT EQUATION

The lift force for the entire wingspan can be calculated using the methodology that follows. From the previous chapter, it was found that a 3-DOF flapping wing model requires the stroke angle (Φ), elevation angle (θ) and angle of attack (α) to be completely defined. It can be postulated that the coefficient of lift is a function of the angle of attack, which in turn is a function of time. Therefore, Equation 3 could be used for normal flight.

It follows that the initial instantaneous lift equation is:

$$L = \frac{1}{2} . \rho . C_l . (V_\infty)^2 . S \qquad (3)$$

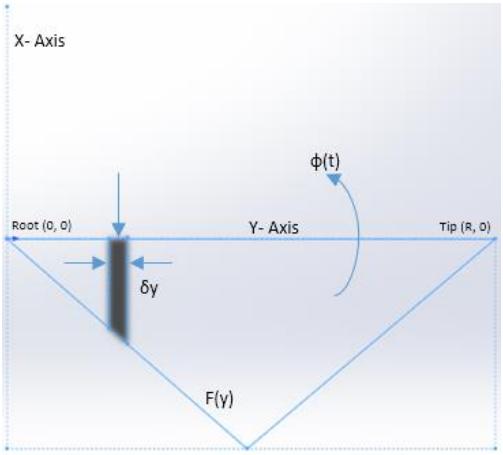

Figure 8: Differential Wing Blade Analysis

From Figure 7 it can be noted that the area of the differential (infinitesimally small) wing segment (for any arbitrary wing blade element) is simply:

$$S = F(y).\delta y \tag{4}$$

The lift equation above can be differentiated with respect to y, to find the lift distribution across the span:

$$(V_\infty)^2 = (r\omega)^2 = y.(\dot{\phi}(t))^2 \tag{5}$$

$$\delta L = \frac{\partial}{\partial y}\left(\frac{1}{2}.\rho.C_l.(V_\infty)^2.S\right) = \frac{1}{2}.\rho.C_l.y^2.(\dot{\phi}^2(t)).F(y)\,dy \tag{6}$$

The lift as a function of time, stroke angle and angle of attack over a wing-beat period can be found by integrating Eq. 6 over the wing span.

$$L = \int_0^R \delta L = \frac{1}{2}.\rho.C_l.(\dot{\phi}^2(t)).I_A \tag{7}$$

where R is the length of the wing

$$I_A = \int y^2 \, dA = \int y^2 \, F(y). \, dy \qquad (8)$$

where I_A is the second moment of inertia

The above lift equation can be used for any wing blade segment, however due to the presence of the second moment of inertia term the wing planform area will be approximated to either a triangular or a rectangular (or a combination of the two).

The drag can be calculated using the same methodology, resulting in the following equation.

$$D = \int_0^R \delta D = \frac{1}{2} . \rho . C_D . (\dot{\phi}^2(t)) . I_A \qquad (9)$$

It is hence noted that the lift and drag are functions of the wing stroke angular velocity and the angle of attack (which are functions of time), as well as a function of the spanwise position (because the second moment of inertia depends on y).

2.2 LIFT EQUATION FOR HOVER

For hovering and vertical takeoff and landing the flapping MAV will experience zero forward velocity, hence a different formulation should be used to understand lift distributions at these states.

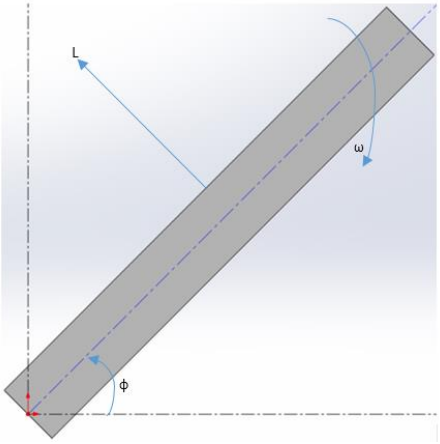

Figure 9: Front View of Wing Blade

This comes about by assuming that during a stroke, the wings sweep with a constant angular velocity of ω between angles of ϕ_0 and $-\phi_0$. Hence, the equation for lift force, for an angle ϕ, is as follows:

$$F(\phi) = 2\int_0^R \cos\phi \frac{1}{2}\rho(\omega x)^2 C_d W\, dx = 2\cos\phi \frac{1}{2}\rho\omega^2 C_d W \frac{R^3}{3} \quad (10)$$

This provides the lift force required for hover and vertical takeoff (with zero forward velocity). It should be noted that W and R represent the dimensions of the wing from the front plane (i.e. the chord and half-span of the wing). Furthermore, a small angle approximation could be made to further simplify this equation, creating a stroke-average lift equation in which lift is constant throughout the stroke angle. This allows for the simplification of terms in the state matrices and control matrices as seen in Chapter 3.

2.3 FLAPPING WING MOTION

To understand the performance of the wings, we looked into previous research that analyzed the relationship between the flapping frequency and lift for the wake capture motion.

Two separate studies were made by Watman and Furukawa where they created a mechanism to test the lift force produced by various wing motions. [16,17]

During their preliminary study in 2008, they examined into the amount of lift the flapping wings can generate for Sinusoidal, Triangular, Trapezoidal and Square wing motion to understand whether the different kinds of motion produce different amounts of lift. Figure 9 shows position and velocity plots for each of the three flapping motions tested.

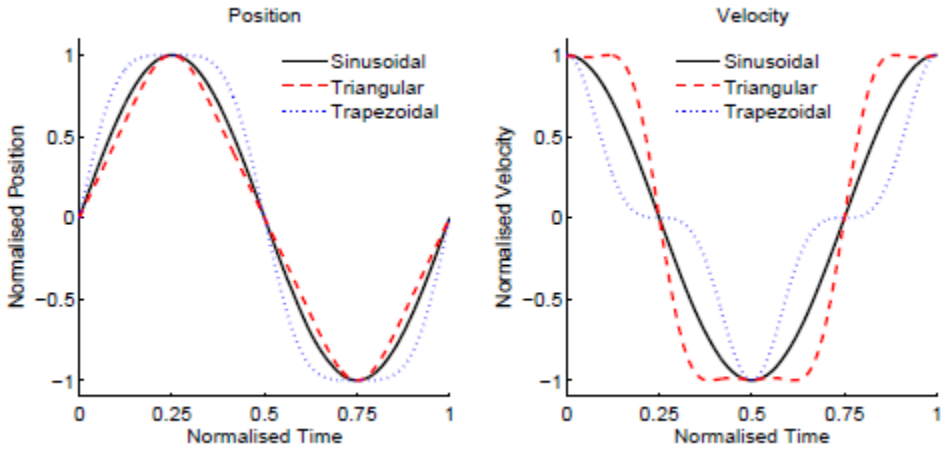

Figure 10: Position and Velocity Plots for the Tested Flapping Motions [Copyright: IEEE Robotics and Automation]

The motions in Figure 9 show that the relative positions of wings are similar, as all three motions return to the center point at nearly the same instant. The biggest difference, however, is the relative velocities. While the sinusoidal is a smooth curve, both the triangular and trapezoidal motions have plateaus in their curves that represent instants at which the wings will stop flapping.

Flapping Motion	Wing Type	Lift (g)	Efficiency (g/W)	Efficiency at $F_{max/2}$ (g/W)
Sinusoidal	A	3.84	**22.22**	14.47
	B	1.89	12.07	8.99
Triangular	A	**4.10**	19.68	**14.94**
	B	2.12	10.17	5.42
Trapezoidal	A	3.21	13.23	7.16
	B	2.28	12.84	8.00

Figure 11: Maximum Values of Performance Measures for Each Wing Type and Flapping Motion [Copyright: IEEE Robotics and Automation]

These results above show that the triangular flapping motion produces the maximum lift force and the highest efficiency at half maximum lift. Because of this we have decided to go with the triangular flapping motion for our wings. While sinusoidal motion gives us a higher efficiency, triangular motion is easier to manufacture and will give us the lift required to get our aircraft into the air.

CHAPTER 3: DESIGN

This section of the report outlines the reasoning behind our design processes and ultimately the final flapping MAV design. Each component went through multiple iterations that satisfied our initial constraints and are optimized based on a lower total weight and maintaining a center of gravity near the location of our measurement unit to avoid having to correct our readings. A summary of the final specifications for the flapping MAV are listed in Table 5.

Specifications for Aircraft	
Wing Span	36 cm
Wing Area	33.75 cm^2
Aspect Ratio	6.67
Flapping Frequency	25 Hz
Height	11.14 cm
Length	7.43 cm
Total Weight	41 g
Payload	0 g
Power	.132 watts

Table 5: Aircraft specifications

3.1 CHASSIS & DRIVETRAIN DESIGN

Based on research conducted, for the proposed design, all of our electronic components were housed in the chassis of the flapping MAV itself. To accomplish this goal we decided to create a chassis and drive train using the SolidWorks software available to use on our campus.

3.1.1 CHASSIS

When considering the chassis design our initial goal was to create a platform within the MAV itself to house all of the electronic components. The design would benefit from being symmetrical to maintain stability within the craft itself and support the weight of all components

during flight. Using these constraints we went through a couple iterations in our conceptual design of the chassis.

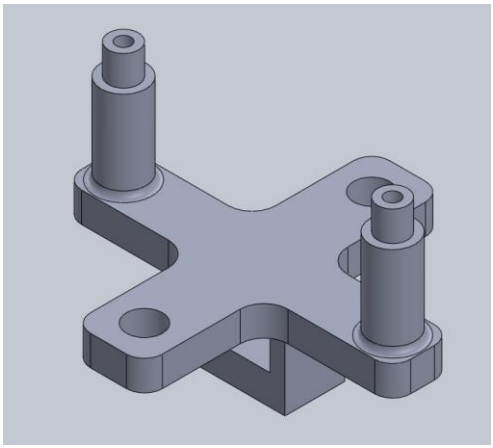

Figure 12: SolidWorks Isometric View of the Chassis

Our initial design involved two separate wing arms that were connected with a separate piece of chassis via epoxy or another adhesive. The design called for the motors to lie on the same plane as the wing arms for a compact set up on the MAV itself. The design as a whole was reconsidered due to concerns about structural integrity. Figure 11 illustrates the final iteration of our chassis design. We decided that having one continuous piece for the central chassis component would withstand the stresses better. This chassis piece also includes plenty of space for us to place the controller and measurement unit on the top face, as well as house the battery in a shelf located on the bottom. The wing arm design was adopted into the new chassis model while the motors were moved to the forward and aft locations on the MAV model to create a cross-shaped chassis piece.

3.1.2 KINEMATIC WHEEL

In order for the motors to work effectively when flapping the wings of the MAV, we needed to manufacture some apparatus to assist the motors. We devised a wheel to linkage system where the motors would turn a 3D printed wheel at the speed necessary to cause the wing to flap. The wheel's design did not change significantly during the iterative process, as the only major edits were the sizing of the lower section to fit over the motor. Figure 12 shows the final design of the wheel.

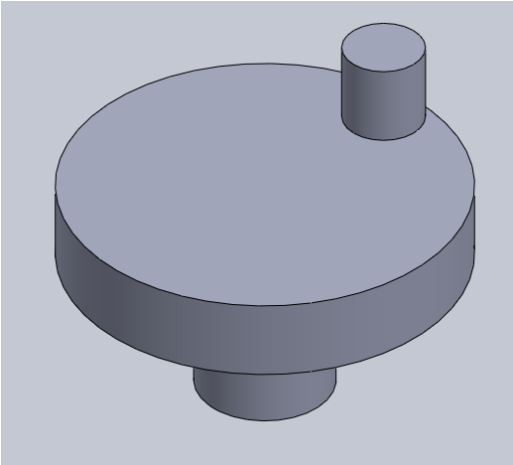

Figure 13: SolidWorks Isometric View of the Wheel

The wheels were constructed with an open tube at the bottom which slides overtop the motor so it will spin at the same speed as the component. The main hub of the wheel would spin a small peg located tangent to the outer rim which fits inside a slider in the wing link. As the wheel spins, the peg moves through the slider and causes the link to pivot on a fixed point where it is connected to the wing arm, thereby causing the wing to flap.

3.1.3 WING LINKAGE

For the MAV to function properly we needed to manufacture a linkage that attaches the wing to the motors that will cause the wing to flap. Like the chassis, these wing links also went through several iterations before deciding on the final design. For all iterations, the links had a small slit where the wing would be located on one end, as well as a slider on the other end where the wheel peg causes the link to turn and the wing to flap.

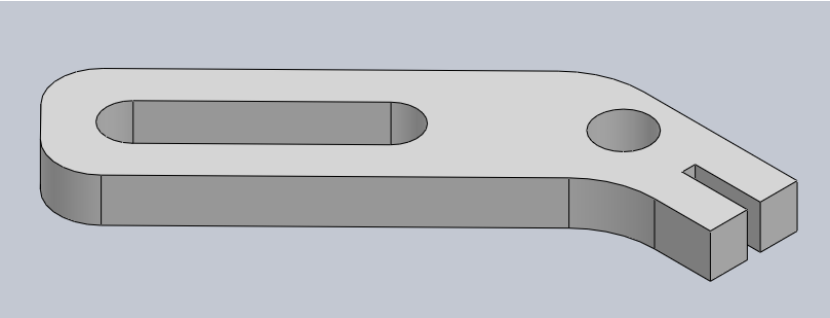

Figure 14: SolidWorks Isometric View of the Link

In the first iteration of the wings, the links were straight when the motors were still lined up on the same axis as the wing arms. After the chassis was updated into the finalized cross pattern, the wing links were bent to account for the motors being offset from the wing arms. Figure 13 shows the final iteration of the wing link. The links still function similarly to their first iteration, which allows the wings a flapping radius of 60 degrees.

3.2 FINAL DESIGN

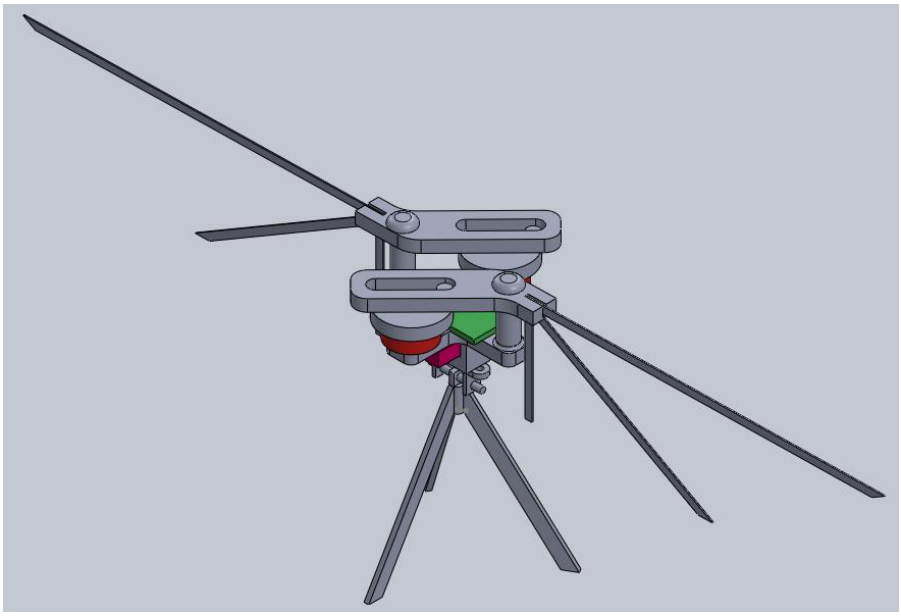

Figure 15: Isometric View of the Flapping Wing MAV

These constraints are very important when attempting to maintain dynamic stability in a state of hover. While keeping these parameters in mind, we were able to construct a design that maintained symmetry about two axes. This has allowed us to simplify the dynamic equations used to model our system and in turn, made our aircraft much easier to control.

Beyond the perspective of our controls system, this symmetry allowed for the placement of the inertial measurement system (IMU) at the center of gravity of the aircraft. This has relevance because if our IMU was not at the center of gravity, we would have to consider our sensor's sensitivity off axes and create time varying transformation matrices to provide us with reliable outputs.

Currently, the MAV has a wingspan of 36.0cm, a weight of 41g and a length of 11cm which satisfy the specifications given at the start of this project.

3.3 PART SPECIFICATION

3.3.1 WINGS

We started by considering the weight of our aircraft using basic laws of motion and particle dynamics to determine how much lift we needed to generate to be able to hover and maintain stable flight.

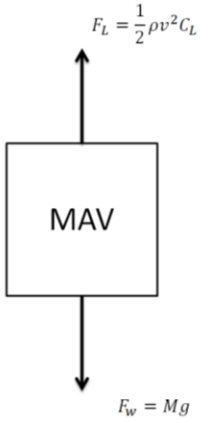

Figure 16: Free-Body Diagram in the Z-Direction (Involving Lift and Weight)

In order to maintain a hover, our aircraft must produce a force of lift equal to the force of gravity acting on the body which is seen in figure 12. After finding the force required, we used these, basic equations for lift, and the typical lift coefficient of small flying animals which is 0.9-1.2, in order to determine the size of the wings and its flapping frequency required to generate lift. We found that wings of 31 cm^2 that beat at 25 Hz would be sufficient for this task.

$$\sum \mathbf{F} = \mathbf{m}\vec{\mathbf{a}} \quad (11)$$

$$\mathbf{C_L} = \frac{\mathbf{L}}{\frac{\mathbf{1}}{\mathbf{2}}\boldsymbol{\rho}\mathbf{v^2}} \quad (12)$$

Because there is no analytical approximation for separated unsteady flow, we feel that the equations above would be a good starting point for our initial calculations and aerodynamic iteration. When applying these force equations, we made the assumption that our wings will be stroking in one plane with the up and down stroke being symmetrical. Using this assumption, we assumed that we can treat each portion of the stroke as a linear translation through stagnant air. From there we proceeded to transform the linear velocity into its rational equivalent to find our wing frequency.

Another important part of this design was the geometry. We decided to go with a triangular wing shape because it represents a semi-elliptical shape while using less material. The elliptic wing shape has been proven, in many tests, to generate a lift distribution that is easy to predict and analyze. It is also one of the most aerodynamically efficient shapes. Although this geometry is usually used for fixed wings, we have seen this wing shape on many small flying animals and are going to see how this style of wing performs using our unsteady flapping motion. This can be seen in figure 15 below.

Figure 17: Hummingbird wing shape [Copyright: mikephoto.com][22]

3.3.2 MOTOR

After researching different types of small electric motors, the brushless motors more appropriate than the brushed motors. Brushless motors have more torque per weight and torque per watt, making them more efficient than their brushed counterparts. They are also more reliable than the brushed motors, which gives them longevity, and do not have to rely on being air-cooled, meaning they can be completely incased within the MAV without worrying about overheating.

With all the parameters above considered, it was not possible to accommodate all the components required for a brushless motor setup due to size constraints. Because brushless motors require a speed controller, the flapping MAV would have to accommodate an extra power supply. Also, speed controllers are generally designed to fit on specific RC aircraft, which are much bigger than ours. Therefore, we picked a brushed motor. A brushed motor contains two magnetic fields that are used to rotate the internal shaft. These motors vary speed using voltage instead of the frequency of alternating current, which is much easier to control, if necessary.

The motor we have selected is a 3.0V geared brushed motor from robotshop.com that weighs 1.2 g and is rated for 1200 KV of power. Although this motor provides a 45% lower KV

(RPM/Volt) than our previous brushless motor, based on our calculations, it shows that we will be able to lift our aircraft due to the 22% weight savings of this redesign. KV is a way that hobbyists classify the power generated by a motor and is what we used to pick the ones for our MAV. This value is a proportion of how fast the unloaded shaft spins divided by the voltage required to attain that angular speed.

Figure 18: 3.0V Robotshop Brushed Motor [Copyright: Robotshop]

3.3.3 TAIL ACTUATOR

When selecting our tail actuator, the main concerns were strength and weight. We performed some calculations for the torque needed to overcome the force of dynamic pressure at the maximum flight speed of 5 m/s. Wind speeds were neglected in these calculations because the purpose of this aircraft is for indoor flight only. We chose a MiniAct 1.1g magnetic actuator from microflight.com because it adequately fulfills this requirement while being extremely lightweight.

Figure 19: MiniAct Magnetic Actuator- 1.1g [Copyright: Plantraco Microflight]

3.3.4 BATTERY

The E-Flite LiPO battery was selected because of its low capacity (of 120 mAh), allowing a current of 0.12A for 1 hour (as is in most RC airplanes and micro-aerial vehicles). According to the datasheet the Arduino Pro-micro that we are using draws 3.3V at 40mA, and we are looking to do a maximum flight demonstration of 2-4 minutes. This battery, however will provide us with an excitation voltage of 3.7V and due to its capacitance, it will provide a maximum theoretical flight time of 3 hours and 5 minutes on a full charge.

Figure 20: E-Flite 120 mAh LIPO Battery [Copyright: SparkFun Inc.]

3.3.5 INERTIAL MEASUREMENT UNIT

When designing the control system for this aircraft, our main priority was being able to maintain dynamic stability at low flight speeds and while hovering. This needed a measurement system that provides high resolution measurements at small perturbations of low speeds. We decided to go with the MPU-6050 from SparkFun. This measurement unit comes complete with a built in 3-axis gyroscope, and 3-axis accelerometer. The system also has an I2C digital output configuration that allows the unit to provide measurements in terms of Euler angles, quaternions,

a rotation matrix, or raw data from an onboard program, which lightens the work load of our main microcontroller.

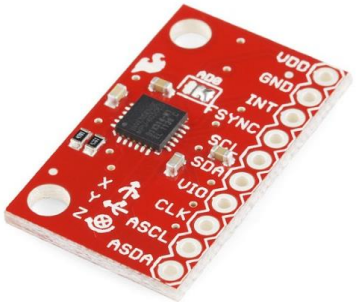

Figure 21: MPU-6050 IMU [Copyright: SparkFun Inc.]

3.3.6 MICROCONTROLLER

After determining the needed specifications of our measurement system, motors, and actuator we now needed a microcontroller that was flexible enough to suit all of our needs. We were able to do this by selecting the 3.3V/ 8MHz Pro Micro microcontroller from sparkfun.com. This controller can receive serial data from our measurement system and adequately power all the aircraft subsystems. Also, something that we strongly considered was how easy it was to program the controller and if it was open-sourced. These traits made an Arduino very attractive; Arduino allows people to post programming techniques for certain components to various online sources.

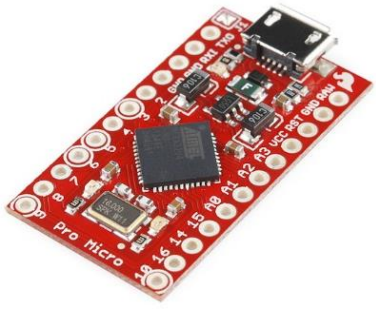

Figure 22: Arduino Pro Micro (3.3V/8MHz) [Copyright: SparkFun Inc.]

CHAPTER 4: MANUFACTURING

This section will discuss the manufacturing processes used to create our MAV and provide insight about the use of unique parts and processes. It deals with the manufacturing processes required to obtain the wings, chassis and drive train.

4.1 WING MANUFACTURING

To attain the rigidity necessary for the wake capturing motion while still keeping the weight down, the wings were chosen to be constructed out of monokote reinforced with carbon fiber strips. To begin, a small sheet of monokote was placed on a flat surface. Two carbon fiber strips were then placed on top of the monokote sheet at a 90 degree angle, which are used as the spars for the wing. The spars are then attached using CA glue to hold them in place while the wing is being constructed. The other half of the sheet of monokote is folded over the top of the carbon fiber strips so the strips are now covered in the plastic material to act as the membrane of the wing.

Once this set up is in place, the monokote is fused together using the process of heat sealing: a hot iron is placed over the sheets of monokote to heat the material past its melting point and then cooled together as one piece of material. During this process the plastic sets around the carbon fiber strips to hold the strips in place. Once the monokote has cooled we used a knife to cut out the shape of the wing around the carbon fiber strips. The final result of this process can be seen in Figure 21.

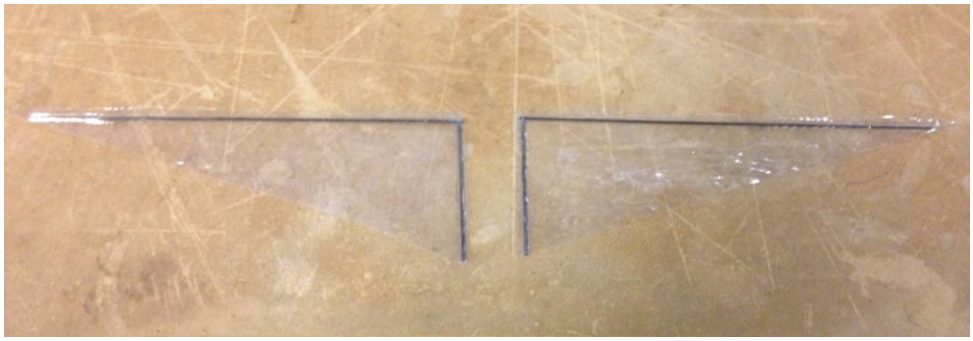

Figure 23: Final Manufactured Wings

4.2 CHASSIS & DRIVETRAIN MANUFACTURING

The chassis, wheels and wing link described above were all first created in its multiple iterations using SolidWorks software so we could easily make changes to the designs as our MAV began to take shape. Once the final designs were decided upon for each piece, we used the Objet Connex350 Multi-Material 3D Printing System on the Worcester Polytechnic Institute campus to print all of the parts. These parts were printed using the VeroWhite material, an opaque plastic that has similar characteristics to acrylonitrile butadiene styrene (ABS), a commonly used thermoplastic. This material was selected for its low density while still having the capacity to hold the weight of the components and wings, giving us a lighter aircraft. These parts would be sanded down in order to make sure that each part fits securely and will not move during flight, and each component will be adhered to the chassis to accomplish this.

CHAPTER 5: VIBRATION ANALYSIS

When considering the material selection for our wings we investigated the natural frequencies of the materials. We did this using the SolidWorks model of the wing and assigned materials to the model for each analysis. Because the carbon fiber material listed in SolidWorks did not have the necessary values to run the analysis, we created our own custom material with the material values for carbon fiber. We used CES EduPack to find the mechanical properties of a carbon fiber matrix similar to the one used in our MAV. Using the Young's Modulus (150 GPa), Poisson's ratio (0.307) and Density (1600 kg/m^3) listed in CES, we have the necessary parameters to run the vibration analysis, with these numbers being based on an epoxy based, laminated matrix carbon fiber which will give us similar properties to the Mylar-coated wings we will be manufacturing. Figure 24 shows the results from the modal analysis.

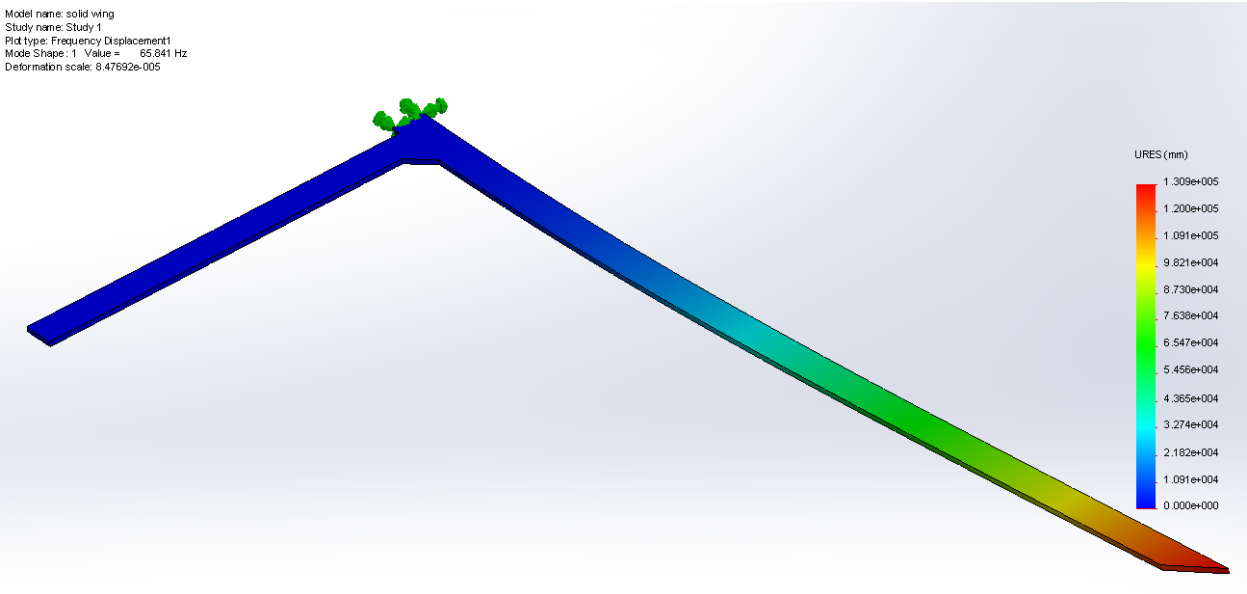

Figure 24: Wing Spar Vibration Testing in SolidWorks

The wing was edited slightly by adding a slight extrusion in the top corner to more accurately represent the wing support forces. The bar on the side of the Figure symbolically represents the displacement experienced by the wing during vibration. For the solid wing we

created a small 3mm width extrusion from the base of the wing spar and created a fixed point at that spot to simulate the wing being connected to the linkage system. From this test we determined that the lowest natural frequency of the wing is 65.8 Hz, which is higher than our testing speed of 25 Hz.

Similar analyses were performed on the Chassis and Wing Link as seen in the Appendix. These parts will be 3D printed using VeroWhite material available at WPI. Because this material shares similar properties to an ABS plastic we used those mechanical properties (Young's Modulus = 2.9 GPa, Poisson's Ratio = .422, Density = 1210 kgm^{-3}) to perform the study. For the chassis, we fixed the forward and aft circular extrusions where the motors will be placed, as well as the underside where the tail is attached, and put two clockwise torque loads on the upper cylinders of the arms to simulate the rotating wing link when it is connected. The lowest natural frequency is 901 Hz, which is again much greater than the testing frequency. For the wing link, we fixed the center circle geometry as well as putting a clockwise centrifugal force inside of it to simulate the interaction with wing arm. The lowest natural frequency is 1202 Hz, which is also much greater than the testing frequency. Through these tests we were able to determine that our parts will not resonate during the testing process.

CHAPTER 6: CONCLUSION & REMARKS

Originally, we wanted to explore the idea of having the MAV achieve full autonomous flight during the testing stage of the project. We investigated utilizing an on board inertial measurement unit to take measurements of the flapping MAV and sending these readings to an on board microcontroller to adjust the subsystems to maintain flight.

It is important that teams recognize there is a need for an in depth practical knowledge for the embedded systems if they plan to make their aircraft autonomous. At WPI, this understanding is best learned through the RBE 3001 course, which covers embedded computing and complex response processes. This would provide students with the knowledge to design a continuous feedback system and its corresponding hardware, which is needed to control an aircraft of this kind. We recommend that students who do not have this knowledge not choose to make their aircraft autonomous.

The use of a radio-controlled (RF) flapping MAV is recommended if the team doesn't have deep robotic knowledge. There are many all-in-one units that enable control of this type of system and many of these packages include multiple servos and motors, a RF receiver, a microcontroller, and power supply. This plug and play type of controller will allow teams to focus on kinematic design, vibrations, and aerodynamics.

Kinematic system design is extremely limited by the manufacturing processes and expertise available at WPI. It is important that teams consider this when designing small, intricate systems. Teams should be prepared to manufacture and assemble this system themselves and should keep that in mind at all steps of the design process.

Aerodynamics of a flapping wing system is very involved and contains many assumptions to reduce the number of degrees of freedom of the system. With that being said, it is important that teams do extensive literature review on the theories surrounding flapping wings and data collected from various tests involving them.

Throughout the 3 terms of this project we have found that it is important to maintain simplicity with initial designs and concepts then, if time and money allow, add complexity to the system. From our experience it is much easier to add sophistication to the project than to attempt to remove it. We began with a very complicated kinematic design for the sake of weight saving s and found that it required manufacturing beyond our skills and budget.

As mentioned above, we recommend that teams stay away from autonomy useless they have extensive practice with embedded systems. Embedded systems is a multidisciplinary topic that requires a thorough understanding of mechanical, electrical, computer and controls engineering.

REFERENCES

1. Zufferey, Jean-Christophe. "The book on Bio-inspired Flying Robots, EPFL Press, 2008, Jean-Christophe Zufferey." The book on Bio-inspired Flying Robots, EPFL Press, 2008, Web. <http://book.zuff.info/>.
2. Thomas J., Mueller. “Fixed and Flapping Wing Aerodynamics for Micro Air Vehicle Applications.” AIAA, 2001. Print.
3. "Sherpa Guides | Chesapeake Bay | Sidebars | Ruby-throated Hummingbird." Sherpa Guides | Welcome to SherpaGuides.com. Web. 31 Aug 2013. <http://www.sherpaguides.com/chesapeake_bay/sidebars/ruby.html>.
4. Wang, Z. Jane. "Dissecting Insect Flight." *Annual Review of Fluid Mechanics.* 37.2005 (2005): 187-190. Print
5. Elimelech, Yossef and Charles P. Ellington. "Analysis of the transitional flow field over a fixed hummingbird wing." *The Journal of Experimental Biology.* (2012): 1-4. Web.<http://jeb.biologists.org/content/early/2012/09/19/jeb.075341. full.pdf>.
6. C.H., Greenwalt. “Dimensional Relationships for Flying Animals.” Smithson Misc., 1962. Print
7. Bruggeman, B., M. Groen, B. Remes and R. Ruijsink. "Improving flight performance of the flapping wing MAV DelFly II." Thesis International Micro Air Vehicle Conference and Competitions (IMAV 2010). (2010): Print
8. Wu, J.C.. "Theory for aerodynamic force and moment in viscous flows." *AIAA Journal.* 19.04 (1981): 432-438. Print
9. Altshuler, D.L., R. Dudley and C.P. Ellington. "Aerodynamic Forces of Revolving Hummingird Wings and Wing Models." Journal of Zoology. 264.(2004): 327-332. Print
10. Nicolara, James , Daniel Pappas and Lucas Sorensen. "Design and Testing of a Flapping Wing Micro Air Vehicle." WPI Major Qualifying Project . (2013): Web.<http://www.wpi.edu/Pubs/E-project/Available/E-project-042313-162648/>.
11. Orlowski, Christopher . "Flapping Wing Micro Air Vehicles: An Analysis of the Importance of the Mass of the Wings to Flight Dynamics, Stability, and Control." The University of Michigan. (2011): Print

12. John D., Anderson Jr.. Fundamentals of Aerodynamics. McGraw-Hill Science/Engineering/Math, 2010. Print.
13. Tobalske, Bret W., Douglas R. Warrick, Christopher J. Clark, Donald R. Powers, Tyson L. Hendrick, Gabriel A. Hyder and Andrew A. Biewener. "Three-dimensional kinematics of hummingbird flight." The Journal of Experimental Biology. 210.(2007): 2368-2382. Print
14. De Croon, G.C.H.E.. "Design, aerodynamics, and vision-based control of the Delfly." International Journal of Micro Air Vehicles. Volume I.Issue II (2009): Print
15. Turnigy Nano-tech 120mAh 2S 25C Lipo Pack (E-flite Micro Series Compatible)." *HobbyKing Store*. N.p., n.d. Web. 03 Oct. 2013. <http://www.hobbyking.com/hobbyking/store/__19422__turnigy_nano_tech_120mah_2s_25c_lipo_pack_e_flite_micro_series_compatible_.html>.
16. Watman, Daniel and Tomonari Furukawa. "A System for Motion Control and Analysis of High-Spped Passively Twisting Flapping Wings." IEEE- Robotics and Automation. (May 19-23, 2008): 1576-1581. Print
17. Watman, Daniel and Tomonari Furukawa. "A Parametric Study of Flapping Wing Performance Using a Robotic Flapping Wing." IEEE- Robotics and Automation. (May 12-17, 2009): 3638-3643. Print
18. "Nature Science Images." National Park Service. Web. <http://www.nps.gov/acad/naturescience/images/raptors9-26.jpg>.
19. Benjamin Y. , Leonard. Flapping Wing Dynamic Modeling. MS Thesis. Virginia Polytechnic Institute and State University, 2011. Print.
20. Nelson, Robert C.. Aircraft Stability and Automatic Control. Third Edition. McGraw-Hill, 1996. Print.
21. Whitney, J.P. and R.J. Wood. "Conceptual Design of Flapping-wing Micro air vehicles." Bioinspiration & Biomimetics. 07.2012 (2012): 1-10. Web.<stacks.iop.org/BB/7/036001>.
22. Lascut, Mike. "Nature Research Photography & Videography." *Where to Photograph Hummingbirds? At Holiday Beach?.* SOTINET INC, 2011. Web. <http://mikephoto.com/where-to-photograph-hummingbirds>.
23. Sane, Sanjay P.. "Steady or Unsteady? Uncovering the Aerodynamics Mechanisms of Insect Flight." *The Journal of Experimental Biology.* Web.<http://jeb.biologists.org/content/214/3/349.full.pdf>.
24. Sane, Sanjay P. and Michael H. Dickinson. "The Control of Flight Force by a Flapping Wing: Lift and Drag Production." The Journal of Experimental Biology. 204.(2001): 2607-2625. Web.<http://jeb.biologists.org/content/204/15/2607.full.pdf>.

APPENDIX A: WEIGHT AND FINANCIAL BUDGET

This appendix shows an Excel chart tracking the weight and financial budget for the project as a whole.

Component	Description	Number	Unit Cost ($)	Combined Cost with Shipping ($)
Battery	E-Flite 120mAh LiPO Battery	1.00	14.90	14.90
Motor	Planetary Gear Pager Motor GM15	2.00	14.25	28.50
Tail Actuator	MiniAct Magnetic Actuator	3.00	6.99	37.55
Accelerometer	Triple-Axis Accelerometer ADXL 335	1.00	24.95	24.95
Gyroscope	Triple-Axis Gyro ITG-3200	1.00	49.95	49.95
Combined IMU Unit	MPU-6050 IMU	1.00	39.95	48.20
Arduino	Arduino Pro Micro (3.3V/8MHz)	1.00	19.95	19.95
Spars	Carbon Fiber, Epoxy	1.00	30.80	38.58
Miscellaneous	Shipping Costs/ Headers/Tools	48.69		48.69
Initial Budget (No.students*$160)				$ 480.00
Total				$ 311.27
Remaining				$ 168.73
Component	**Description**	**Number**	**Unit Weight (g)**	**Combined Weight (g)**
Battery	E-Flite 120mAh LiPO Battery	1	3.4	3.4
Motor	Park 180 Outrunner Motor	2	1.2	2.4
Tail Actuator	MiniAct Magnetic Actuator	1	1.1	1.1
Combined IMU Unit	MPU-6050 IMU	1	1.6	1.6
Arduino	Arduino Pro Micro (3.3V/8MHz)	1	1.9	1.9
Wings	Carbon Fiber Reinforced Monokote	2	0.7	1.4
Chassis	3D printed VeroWhite Chassis	1	10	10
Wheels	3D printed VeroWhite Wheels	2	3.1	6.2
Links	3D printed VeroWhite Links	2	3.9	7.8
Peg	3D printed VeroWhite Pegs	2	0.1	0.2
Tail	3D printed VeroWhite Tail	1	5	5
Total Combined Weight (g)				**41**

APPENDIX B: SOLIDWORKS DRAWINGS AND ANALYSES

This appendix shows the drawings in SolidWorks of each part that was 3D printed or manufactured as well as the frequency analysis tests done that were referenced in Chapter 3 but were not located within the report.

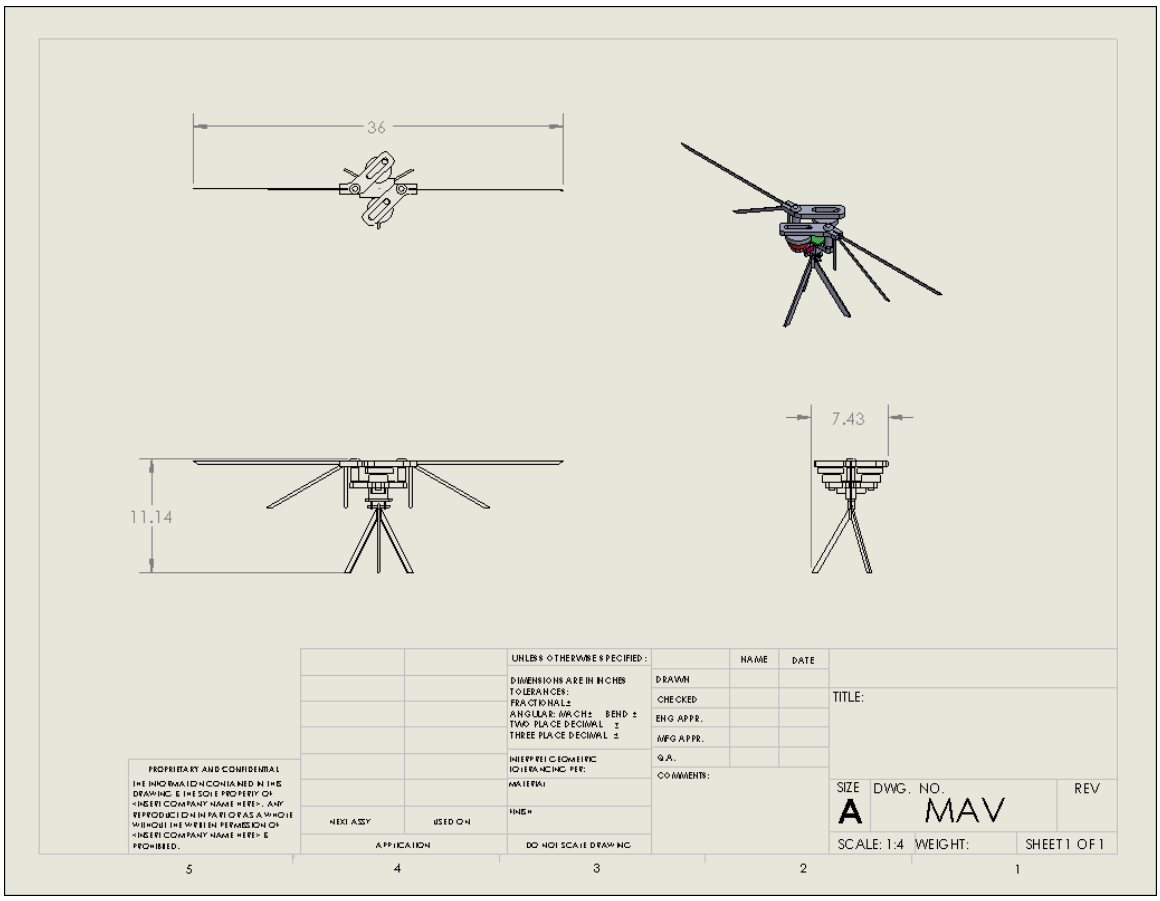

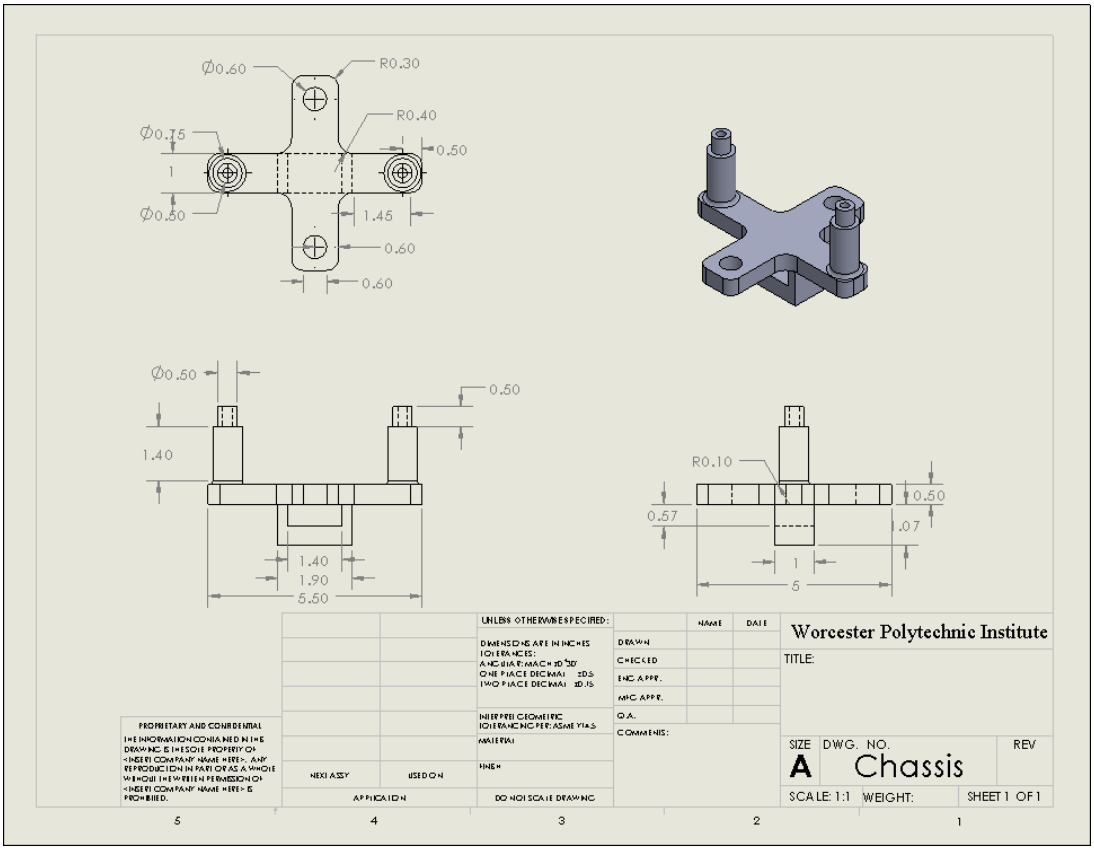
Ø0.60
R0.30
R0.40
Ø0.75
0.50
1
Ø0.50
1.45
0.60
0.60
Ø0.50
0.50
1.40
1.40
1.90
5.50
R0.10
0.50
0.57
.07
1
5
Worcester Polytechnic Institute
TITLE:
SIZE
A
DWG. NO.
Chassis
REV
SCALE: 1:1
WEIGHT:
SHEET 1 OF 1

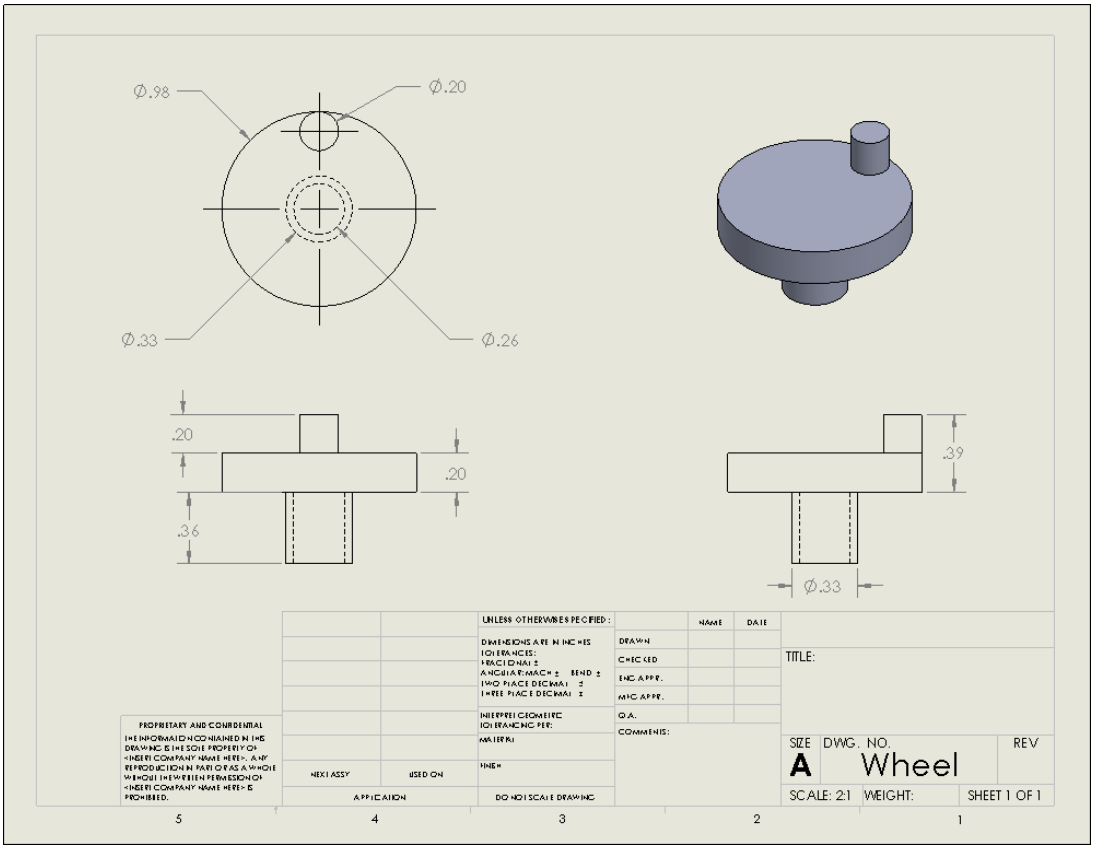
Ø.98
Ø.20
Ø.33
Ø.26
.20
.20
.36
.39
Ø.33
TITLE:
SIZE
A
DWG. NO.
Wheel
REV
SCALE: 2:1
WEIGHT:
SHEET 1 OF 1

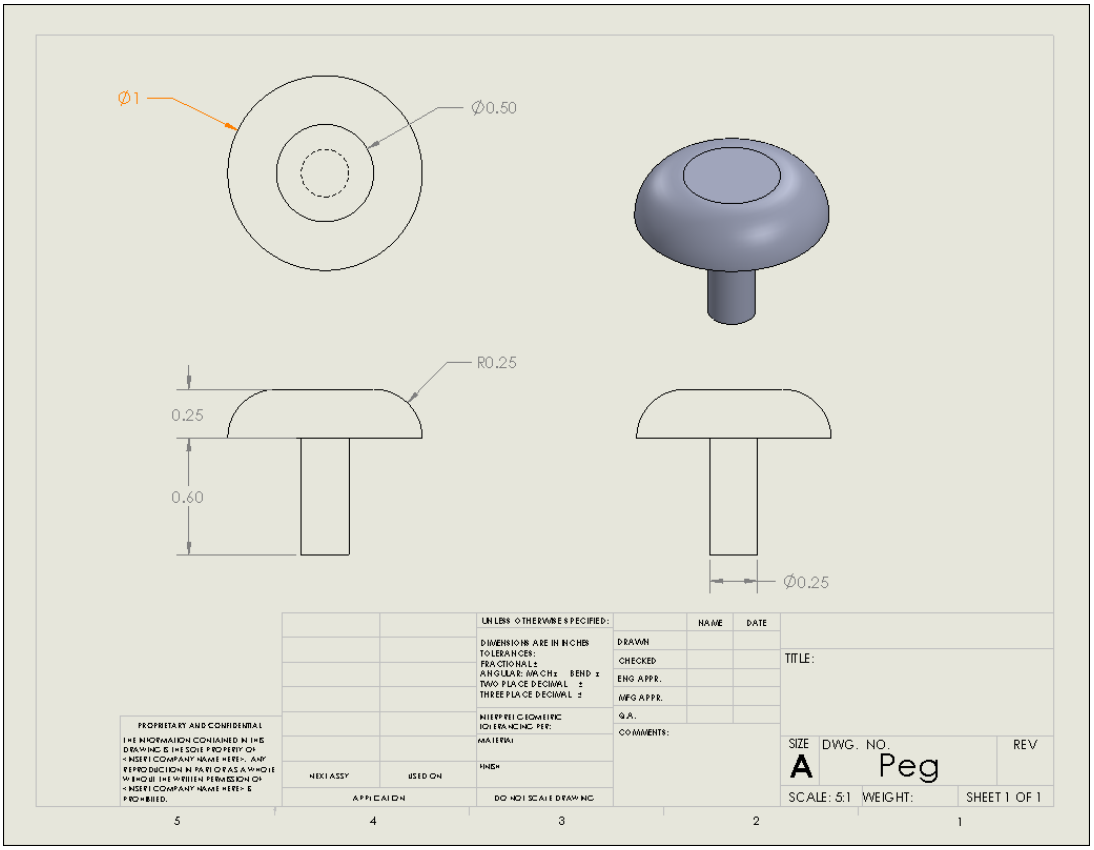
Ø1
Ø0.50
R0.25
0.25
0.60
Ø0.25
UNLESS OTHERWISE SPECIFIED:
DIMENSIONS ARE IN INCHES
TOLERANCES:
FRACTIONAL ±
ANGULAR: MACH ± BEND ±
TWO PLACE DECIMAL ±
THREE PLACE DECIMAL ±
INTERPRET GEOMETRIC TOLERANCING PER:
MATERIAL
FINISH
NEXT ASSY
USED ON
APPLICATION
DO NOT SCALE DRAWING
NAME
DATE
DRAWN
CHECKED
ENG APPR.
MFG APPR.
Q.A.
COMMENTS:
TITLE:
PROPRIETARY AND CONFIDENTIAL
THE INFORMATION CONTAINED IN THIS DRAWING IS THE SOLE PROPERTY OF <INSERT COMPANY NAME HERE>. ANY REPRODUCTION IN PART OR AS A WHOLE WITHOUT THE WRITTEN PERMISSION OF <INSERT COMPANY NAME HERE> IS PROHIBITED.
SIZE
A
DWG. NO.
Peg
REV
SCALE: 5:1
WEIGHT:
SHEET 1 OF 1

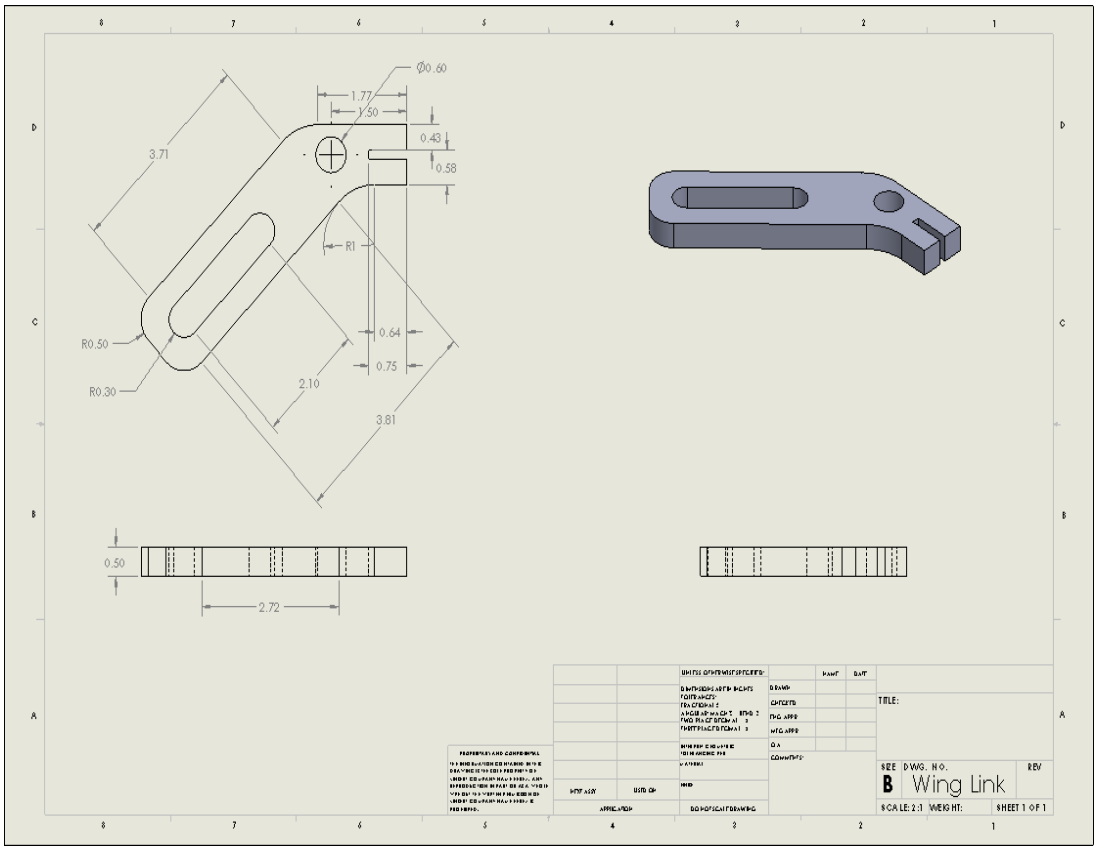
Ø0.60
1.77
1.50
0.43
0.58
3.71
R1
R0.50
R0.30
0.64
0.75
2.10
3.81
0.50
2.72
UNLESS OTHERWISE SPECIFIED:
DRAWN
CHECKED
ENG APPR.
MFG APPR.
Q.A.
COMMENTS:
NAME
DATE
TITLE:
SIZE
B
DWG. NO.
Wing Link
REV
SCALE: 2:1
WEIGHT:
SHEET 1 OF 1

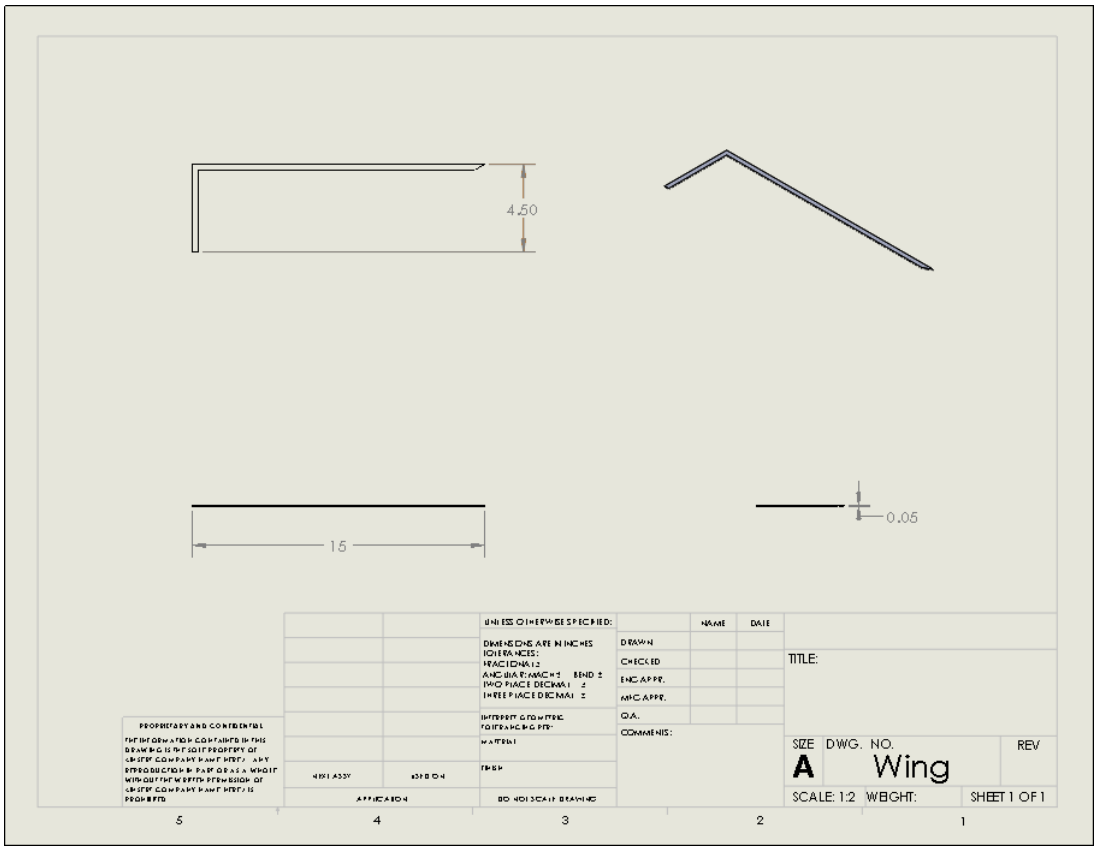
4.50
15
0.05
UNLESS OTHERWISE SPECIFIED:
DIMENSIONS ARE IN INCHES
TOLERANCES:
FRACTIONAL ±
ANGULAR: MACH ± BEND ±
TWO PLACE DECIMAL ±
THREE PLACE DECIMAL ±
INTERPRET GEOMETRIC TOLERANCING PER:
MATERIAL
FINISH
NEXT ASSY
USED ON
APPLICATION
DO NOT SCALE DRAWING
NAME
DATE
DRAWN
CHECKED
ENG APPR.
MFG APPR.
Q.A.
COMMENTS:
TITLE:
SIZE
A
DWG. NO.
Wing
REV
SCALE: 1:2
WEIGHT:
SHEET 1 OF 1
PROPRIETARY AND CONFIDENTIAL
THE INFORMATION CONTAINED IN THIS DRAWING IS THE SOLE PROPERTY OF <INSERT COMPANY NAME HERE>. ANY REPRODUCTION IN PART OR AS A WHOLE WITHOUT THE WRITTEN PERMISSION OF <INSERT COMPANY NAME HERE> IS PROHIBITED.
5
4
3
2
1